Conduction-combined forced and natural convection in a lid-driven parallelogram-shaped enclosure divided by a solid partition

Ali J. Chamkha*

Manufacturing Engineering Department,
The Public Authority for Applied Education and Training,
P.O. Box 42325, Shuweikh 70654, Kuwait
E-mail: achamkha@yahoo.com
*Corresponding author

Salam Hadi Hussain and Farooq Hassan Ali

Mechanical Engineering Department,
College of Engineering,
Babylon University,
Babylon Province, Iraq
E-mail: salamphd1974@yahoo.com
E-mail: farooq_hassan77@yahoo.com

Ahmed Ali Shaker

Mechanical Engineering Department,
College of Engineering,
AI-Qadissiya University,
AI-Qadissiya Province, Iraq
E-mail: ahmedalsaadi78@gmail.com

Abstract: Conduction-combined forced and natural convection heat transfer flow of air in a differentially heated lid-driven parallelogram-shaped enclosure divided by a solid partition has been formulated and solved numerically using the finite-volume method with the SIMPLE algorithm. For the two-dimensional problem, numerical solutions are obtained for a wide range of Richardson numbers ($0.1 \leq Ri \leq 10$), inclination angles of enclosure from the vertical direction ($-60° \leq \Phi \leq 60°$), and thermal conductivity ratios ($0.001 \leq K \leq 10$). The results indicate that all of the studied parameters and direction of moving lid have significant effects on Nusselt number and the average skin friction coefficient.

Keywords: mixed convection; conjugate; lid-driven enclosure; parallelogram; partition; finite volume.

Reference to this paper should be made as follows: Chamkha, A.J., Hussain, S.H., Ali, F.H. and Shaker, A.A. (2012) 'Conduction-combined forced and natural convection in a lid-driven parallelogram-shaped enclosure divided by a solid partition', *Progress in Computational Fluid Dynamics*, Vol. 12, No. 5, pp.309–321.

Biographical notes: Ali J. Chamkha is a Professor in the Manufacturing Engineering Department, College of Technological Studies at the Public Authority for Applied Education and Training in Kuwait. He earned his PhD in Mechanical Engineering from Tennessee Technological University, USA, in 1989. His research interests include multiphase fluid-particle dynamics, fluid flow in porous media, heat and mass transfer, magnetohydrodynamics and fluid particle separation. He has served as an Associate Editor for *Fluid/Particle Separation Journal* and *International Journal of Energy and Technology*. He has authored and co-authored over 300 papers in archival journals and conferences.

Salam Hadi Hussain is a member at the Mechanical Engineering Department in the University of Babylon, Hilla, Iraq. He received his PhD in Mechanical Engineering from Baghdad University in 2005. His research work concerns numerical and experimental analysis and application of heat transfer and fluid flow in nano-systems, porous media, magnetohydrodynamics and fluid particle separation, refrigeration and air-conditioning systems and other areas of thermal and fluid sciences. He has published several international journals and conference papers on these topics.

Farooq Hassan Ali is a member at the Mechanical Engineering Department in the University of Babylon, Hilla, Iraq. He received his Master's Degree from Babylon University in 2001. His research interest is fluid dynamics and heat transfer. He has published several papers in archival journals on these topics.

Ahmed Ali Shaker earned his MSc in Mechanical Engineering – Power (Heat Transfer). He is a member in Mechanical Engineering Department, College of Engineering, Al-Qadisiya University, Iraq. His research interests include heat and mass transfer, computational fluid dynamics and applied mechanics. He has published several papers in archival journals (*Developing Laminar Flow, Free Convection Heat Transfer*, *Design of Jack and Disturbed Flow*).

1 Introduction

Mixed convection in an enclosure is relevant to many environmental applications such as cooling of electronics, air solar collectors, furnaces design, nuclear reactors and building applications. Very little studies have been reported for lid-driven parallelogram-shaped enclosure. Few authors dealt with natural convection in parallelogramic enclosures (Nakumura and Asako, 1980, 1982, 1984; Naylor and Oosthuizen, 1994; Costa, 2004a, 2004b; Costa et al., 2005). Bairi et al. (2010) carried out a numerical study of the transient natural convection in parallelogramic cavities with two vertical active walls maintained at different temperatures while the inclined walls were adiabatic. The authors presented the temperature fields and the flow lines at some reprehensive instants of the transient state for all angles treated. Garcia et al. (2010) complemented the study on high Rayleigh number convection regime in parallelogramic cavities. The variations in the mean Nusselt number were presented as a function of the inclination angle and Rayleigh number. Oztop and Varol (2009) and Oztop et al. (2009a) investigated the flow field, temperature distribution and heat transfer in a porous media filling lid-driven cavity and examined the effect of inserted circular-shaped body into lid-driven enclosure on mixed convection heat transfer. Ben Nakhi and Chamkha (2006) investigated laminar, two-dimensional natural convection owing to sidewalls temperature gradient inside an inclined partitioned enclosure. The upper and bottom walls were assumed to be insulated. Three repetitive partitions existed along the bottom wall of the major enclosure. Jae and Man (2006) considered a physical model consisting of a horizontal layer of fluid heated below and cold above with a heat-generating conducting body placed at the centre of the layer. The results for the case of conducting body with heat generation were compared with those without heat generation to study the effects of heat generation from the conducting body on the fluid flow and heat transfer in the enclosure. Mahapatra et al. (2007) studied numerical simulation of mixed convection in a differentially heated square enclosure with a partition. The phenomenon inside the enclosure with centrally located partitions and offset partitions was also analysed for the isotherm and streamline patterns and shielding effect of such partitions. Oztop et al. (2009b) studied the conduction-combined forced and natural convection (mixed convection) heat transfer and fluid flow for 2D lid-driven square enclosure divided by a partition with a finite thickness and finite conductivity. The horizontal walls were considered adiabatic while the two vertical walls were maintained at isothermal temperatures. This investigation covered a wide range of values of the Richardson number, which was changed from 0.1 to 10 and the thermal conductivity ratio varied from 0.001 to 10. A wide range of Richardson numbers was explored also encompassing the stability limit for 2D, laminar, steady regimes. It was observed that though orientation of the moving lid could not affect the direction of flow at the right chest, it completely affected the flow field at the left chest. The mean Nusselt number decreased with increasing values of the Richardson number for all values of the thermal conductivity ratio. For low Richardson numbers ($Ri = 0.1$), forced convection played a dominant role in convection and the mean Nusselt numbers for all values of the thermal conductivity ratio were almost the same. The heat transfer decreased with increasing values of the thermal conductivity ratio for all Richardson number values. Oztop et al. (2009c) investigated the natural convection in a vertically divided square enclosure by a solid partition into air and water regions. Thus, two cases were examined: left side of partition was filled with air and right side was filled with water. It was found that flow field, temperature distribution and heat transfer were affected by the changing of filled fluid in the chests. When the left chest was filled with air, higher heat transfer was obtained. Varol et al. (2010) made a numerical analysis of conduction-natural convection in inclined divided enclosures filled with different fluids. One side of the partition of enclosure was filled with air and the other side was filled with water. The enclosure was heated from one vertical wall and cooled from the other while horizontal walls were adiabatic. The results showed that the heat transfer was lower on the air side of the enclosure than that on the water side. Zaho et al. (2010) examined the inverse heat transfer problem in an enclosure simultaneously involving natural convection and heat conduction, which was still unexplored although it was significant for flow control to simultaneously involve heat conduction and convection regimes.

The previous studies clearly show that lid-driven differentially heated cavities with partitions have interesting applications in various fields and the conduction-combined forced and natural convection heat transfer in a differentially heated lid-driven parallelogram-shaped enclosures have not been reported yet. Depending on the applications, various interactions between conduction and combined forced and natural convection should be known. The purpose of the current work is to solve numerically two-dimensional conduction-combined convection flow equations in a lid-driven parallelogram-shaped cavity filled with air and divided by a solid partition wall. The cavity is cooled from the right side and heated from the left wall. Also, the left wall is considered to be sliding upward or downward at a constant velocity. The current model is based on the geometry of Oztop et al. (2009b), for a left vertical heated moving lid and right vertical cooled stationary wall cavity, which is divided by a vertical centred solid partition filled with air (Pr = 0.71). Numerical solutions are obtained over a wide range of Grashof numbers ($10^4 \leq \mathrm{Gr} \leq 10^6$) with the Reynolds number kept fixed at 316.227. The current work solves the same problem, but in this situation, a lid-driven parallelogram-shaped cavity is used instead of a square cavity.

2 Model specification and mathematical formulation

The physical model considered in this work along with the important geometric parameters is shown in Figure 1. A cartesian coordinate is used with the origin at the lower left corner of the computational domain. The physical model is a parallelogramic cavity that includes a divider with finite length (H) and thermal conductivity (k_S). The height of the cavity is shown by H and the width of cavity is W. The partition is located at the centre of the enclosure and the thickness of the cavity is taken as constant such that $S = W/10$. Both the left moving wall and the right stationary vertical walls are inclined at an angle (Φ) with respect to the vertical and isothermal but temperature of the left wall is higher than that of the right wall. However, the horizontal walls are adiabatic. The left side of the parallelogramic cavity moves at an angle of (Φ) in $+y$ or $-y$ in the inclined direction. The effect of various orientations on the heat transport process inside the parallelogramic cavity is studied in this work. It is necessary to examine the range of the governing parameters Re and Ri chosen in this study. To maintain laminar flow in the cavity, the value of Re is kept fixed at 316.227 and Ri considered in the range 0–10 over a wide range of Grashof numbers ($10^4 \leq \mathrm{Gr} \leq 10^6$) and the Prandtl number Pr is taken as 0.71. The obtained numerical results are presented graphically in terms of isotherm and streamline maps to illustrate the interesting features of the solution. The fluid properties are also assumed to be constant, except for the density in the buoyancy term, which follows the Boussinesq approximation. The radiation effects are neglected and the gravitational acceleration acts in the negative y-direction. The fluid within the cavity is assumed to be Newtonian while the viscous dissipation effects are considered negligible. The viscous incompressible flow and the temperature distribution inside the parallelogram cavity are described by the Navier–Stokes and energy equations, respectively. The governing equations are transformed into a dimensionless form by using the following non-dimensional variables as given by Rahman et al. (2008):

$$\theta = \frac{T - T_c}{T_h - T_c},\ \theta_s = \frac{T_s - T_c}{T_h - T_c},\ X = \frac{x}{H},\ Y = \frac{y}{H},$$
$$U = \frac{u}{V_p},\ V = \frac{v}{V_p},\ P = \frac{p}{\rho V_p^2},\ \Pr = \frac{\vartheta}{\alpha},\ \mathrm{Re} = \frac{V_p H}{\vartheta},$$
$$Gr = \frac{g\beta(T_h - T_c)H^3}{\vartheta^2} \quad \text{and } \mathrm{Ri} = \frac{Gr}{\mathrm{Re}^2} \tag{1}$$

where X and Y are the dimensionless coordinates measured along the horizontal and vertical axes, respectively, u and v being the dimensional velocity components along x and y axes, respectively, and θ is the dimensionless temperature, β is the volumetric coefficient of thermal expansion and g is the gravitational acceleration. The dimensionless forms of the governing equations under steady-state condition are expressed in the following forms (Rahman et al., 2008):

$$\frac{\partial U}{\partial X} + \frac{\partial V}{\partial Y} = 0 \tag{2}$$

$$U\frac{\partial U}{\partial X} + V\frac{\partial V}{\partial Y} = -\frac{\partial P}{\partial X} + \frac{1}{\mathrm{Re}}\left(\frac{\partial^2 U}{\partial X^2} + \frac{\partial^2 U}{\partial Y^2}\right) \tag{3}$$

$$U\frac{\partial V}{\partial X} + V\frac{\partial V}{\partial Y} = -\frac{\partial P}{\partial Y} + \frac{1}{\mathrm{Re}}\left(\frac{\partial^2 V}{\partial X^2} + \frac{\partial^2 U}{\partial Y^2}\right) + \mathrm{Ri}\,\theta \tag{4}$$

$$U\frac{\partial \theta}{\partial X} + V\frac{\partial \theta}{\partial Y} = \frac{1}{\mathrm{Re}\,\mathrm{Pr}}\left(\frac{\partial^2 \theta}{\partial X^2} + \frac{\partial^2 \theta}{\partial Y^2}\right). \tag{5}$$

For the heat-conducting partition, the energy equation is

$$\left(\frac{\partial^2 \theta_s}{\partial X^2} + \frac{\partial^2 \theta_s}{\partial Y^2}\right) = 0. \tag{6}$$

The Richardson number Ri ($\mathrm{Gr}/\mathrm{Re}^2$), which appears in last term of equation (4), characterises the mixed convection flow where Gr and Re represent the strength of the natural and forced convection effects, respectively. As $\mathrm{Ri} \to 0$, the heat transfer regime is governed by forced convection, and as $\mathrm{Ri} \to \infty$, the natural convection regime becomes dominant. The governing parameters are the Richardson number Ri, which changes between 0 and 10, the thickness ratio of the partition to the wall S/H, which is set to 0.1, and the conductivity ratio $K = k_f/k_S$, which is varied as $K = 0.001, 1, 10$.

Figure 1 Schematic diagram and coordinate system of the physical domain with boundary conditions

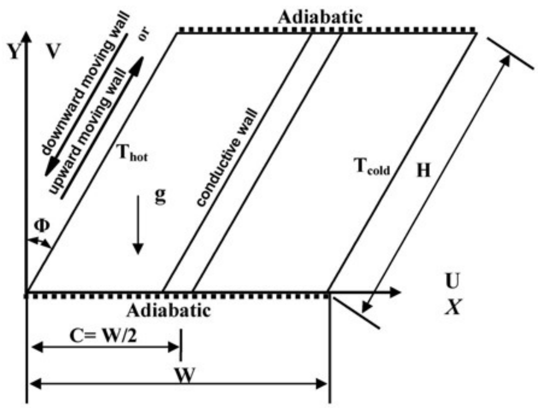

The non-dimensional form of the boundary conditions for the present problem is specified as follows:

On moving wall: $X = 0$, $0 \le Y \le 1$; $U = 0$, $V = 1$ (for upward moving lid), $U = 0$, $V = -1$ (for downward moving lid), $\theta = 1$.

On right vertical wall: $X = 1$, $0 \le Y \le 1$; $U = 0$, $V = 0$, $\theta = 0$.

On the bottom and top walls: $U = 0$, $V = 0$, $\dfrac{\partial\theta}{\partial Y} = 0.$

At all solid boundaries: $U = 0$, $V = 0$.

At the solid–fluid vertical interfaces of the block: $\left(\dfrac{\partial\theta}{\partial X}\right)_{\text{fluid}} = K\left(\dfrac{\partial\theta}{\partial X}\right)_{\text{solid}}.$

At the solid–fluid horizontal interfaces of the block: $\left(\dfrac{\partial\theta}{\partial Y}\right)_{\text{fluid}} = K\left(\dfrac{\partial\theta}{\partial Y}\right)_{\text{solid}}.$

The average Nusselt number $(\overline{\text{Nu}})$ at the moving hot left wall is as given by Oztop et al. (2009b):

$$\overline{\text{Nu}} = \int_0^1 \frac{(\partial\theta/\partial X)_W}{(\partial\theta/\partial X)_{\text{Cond}}}\,\text{d}Y. \tag{7}$$

Note that $(\partial\theta/\partial X)_{\text{Cond}}$ is the temperature gradient without a partition. The skin friction coefficient, $C_f(Y)$, at the moving hot left wall is also a quantity of interest in this study for estimating the total drag force on the surface. This is calculated as

$$C_f(Y) = \mu(\partial U/\partial X)_{x=0} / (\rho V_{\text{Lid}}^2 / 2). \tag{8}$$

To examine the effect of the hot left wall velocity and the hot left wall inclination angle from the vertical (Φ) for the parallelogramic cavity on the overall flow and heat transfer process, the average skin friction coefficient (viscous drag coefficient) C_f at the moving hot left wall is also calculated by integrating $C_f(Y)$ over the length of the hot left wall as follows:

$$C_f = \int_0^1 C_f(Y)\,\text{d}Y. \tag{9}$$

Simpson's 1/3 rule is used for numerical integration to obtain the average Nusselt number and the average skin friction coefficient.

3 Computational procedure

This computational investigation is based on the finite-volume method to discretise the governing non-dimensional equations as discussed by Patankar (1980). Non-staggered grid procedure is used in primitive variables with a power-law differencing scheme and a second-order central differencing scheme for convection and diffusion terms for the fluid domain. Computing on a collocated grid requires computing the cell face velocities, which are needed. The SIMPLE algorithm is utilised to handle the pressure, temperature and velocity coupling of governing equations. The pressure correction equation is derived from the continuity equation to enforce the local mass balance. Linear interpolation and numerical differentiation as given by Ferzinger and Peric (1999) are used to express the cell-face value of the variables and their derivatives through the nodal values. The method is applied to conjugate problem by employing ghost nodes at the fluid–solid interface as described by WanLai et al. (1997) and Liaqat and Baytas (2001). In this method, the flow in the cavity and conduction in the walls are solved simultaneously. This is achieved by employing the ghost nodes at the fluid–solid interface, as shown in Liaqat and Baytas (2001). The final discredited form of governing equations is solved iteratively using Stone's SIP solver (Stone, 1968). Iteration is continued until difference between two consecutive field values of variables is less than or equal to 10^{-6}. For further stabilisation of numerical algorithm, underrelaxation factors of 0.2–0.85 are used. The description of this solution method is given in detail by Ferzinger and Peric (1999) and the details are not repeated herein for brevity.

4 Grid refinement check

To obtain a grid-independent solution, a grid refinement study is performed for a parallelogramic cavity that includes a divider with finite thickness ($S = W/10$) and conductivity (k_S) with the horizontal adiabatic walls. Both the left moving vertical wall and the right stationary vertical wall are inclined at an angle of (Φ) with respect to the vertical direction and are isothermal with the temperature of the left wall being higher than that of the right wall. For the same boundary conditions of the current study with Ri = 10, Φ = 60°, Pr = 0.71 and $K = 10$, eight combinations (40 × 40, 50 × 50, 60 × 60, 70 × 70, 80 × 80, 100 × 100, 120 × 120 and 150 × 150) of non-uniform grids are used to test the effect of grid size on the accuracy of the predicted results.

High-density grids are employed near the fluid–solid interface to resolve the boundary layer properly. The density of the grids is higher near the walls where sharp gradients of temperature and velocity are expected. Figure 2 shows the convergence of the average Nusselt number $(\overline{Nu})$ at the upward moving left inclined side wall of the parallelogramic cavity with grid refinement. It is observed that grid independence is achieved with combination of (100×100) control volumes where there is insignificant change in the average Nusselt number $(\overline{Nu})$ with the improvement of finer grid. The agreement is found to be excellent, which validates the present computations indirectly. However, a relatively finer mesh combination (100×100) has been adopted for the whole set of the current simulations.

Figure 2 Convergence of average Nusselt number along the upward moving left inclined side wall of the parallelogram-shaped enclosure with grid refinement for Ri = 10, Φ = 60°, Pr = 0.71 and K = 10

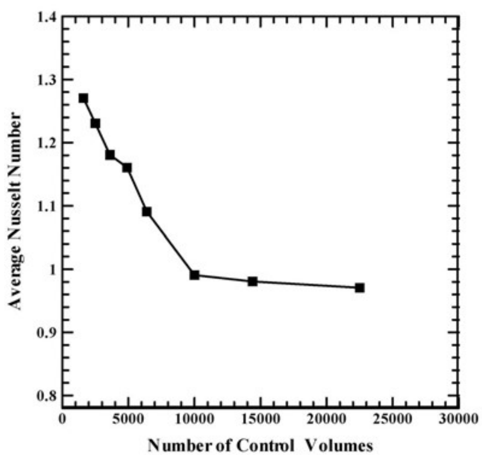

5 Numerical results verification

To make sure that the developed programs are free of errors, a verification test is conducted. The present numerical approach is verified against the results published by Oztop et al. (2009b) for natural convection in a square cavity of dimensions $L \times L$ that includes a divider with finite thickness ($S = W/10$) and thermal conductivity (k_S) with the horizontal adiabatic walls. Both the left downward moving wall and the right stationary vertical walls are isothermal but the temperature of the left wall is higher than that of the right wall. The calculated surface-averaged Nusselt numbers along the moving left wall for the two test cases (upward and downward moving lid) are compared with the benchmark values by Oztop et al. (2009b) as shown in Table 1. Figure 3 shows the streamlines and isotherms calculated by Oztop et al. (2009b) and by this study for different Richardson numbers Ri changing from (a) Ri = 0.1, (b) Ri = 1, (c) Ri = 10 with Gr = 10^5, Pr = 0.71, $K = 1$, $C = 0.5$ and $\Phi = 0°$ using the same boundary conditions but the numerical scheme is different. Excellent agreement is achieved between the results of Oztop et al. (2009b) and the present numerical scheme for both the streamline and temperature contours inside the square cavity as shown in Figure 3. These verifications created a good confidence in the present numerical model to deal with the physical problem.

Table 1 Comparison of the results of average Nusselt number along moving wall for validation with two different cases at Pr = 0.71, Gr = 10^5 and Φ = 0°

Case	*Source data results*	*Ri*	*Mean Nusselt number along moving wall* *K = 0.001*	*K = 1*	*K = 10*	*Max. error* (%)
Upward moving lid	Oztop et al. (2009b) results	0.1	2.8400	2.020000	0.67000	–1.90
		1	2.5500	2.030000	0.66000	
		10	2.25000	1.850000	0.64000	
	Present work results	0.1	2.88478	2.053250	0.66525	
		1	2.57241	2.041025	0.65589	
		10	2.27085	1.866580	0.62784	
Downward moving lid	Oztop et al. (2009b) results	0.1	2.82000	2.020000	0.67000	–1.9947
		1	2.02000	1.700000	0.66000	
		10	1.63000	1.410000	0.57000	
	Present work results	0.1	2.84533	2.044300	0.67781	
		1	2.03142	1.725840	0.65905	
		10	1.64210	1.422310	0.55863	

6 Results and discussion

Numerical analysis has been performed to investigate the flow field and temperature distribution in parallelogramic lid-driven cavity divided by a solid conductive partition. The ranges of parameters considered in this study are $(0.1 \le \text{Ri} \le 10)$, $(10^4 \le \text{Gr} \le 10^6)$, $(0.001 \le K \le 10)$ and $(-60° \le \Phi \le 60°)$. All results are obtained for Pr = 0.71 because the most likely applications are for air.

Figure 4 shows the isotherms (on the left) and streamlines (on the right) for different Richardson numbers and thermal conductivity ratios. For the case where the lid is moving upward, the flow structure is characterised by a primary recirculating clockwise cell that occupies the left chest. The flow rises by the moving lid and impinges on the top wall and the partition then rotates in clockwise direction to the bottom wall. The flow rotation in the right chest is in the same direction of flow as in the left chest, which is produced by pure natural convection, where the fluid near the right side of the partition is heated and has lower density, moves to upward direction while the fluid near the right wall is cooled and, therefore, it moves downward. With increasing values of the Richardson number, the effect of natural convection in the left chest appears through the flow circulation centre, which moves to the centre of the chest. By increasing the thermal conductivity ratio, no effect on the flow structure is noticed especially at $K = 0.001$, 1 and the main change occurs when $K = 10$ because of the corresponding decrease in the thermal resistance. The isotherms for this case show that the hottest region occurs in the left chest and is concentrated at the bottom left and top right sides of the left chest. The strength of the hot region increases with increases in the value of the Richardson number because of the opposite effect of force and natural convection. Increasing the value of the thermal conductivity ratio shows that the isothermal lines are spread into the two chests and become more uniformly distributed because the thermal resistance of the partition decreases. In the case of downward lid-driven motion, one primary and another secondary cells are formed in the left chest. For $K = 0.001$, the primary cell is formed owing to the force of buoyancy and moves in the clockwise direction while the secondary cell is formed owing to forced convection and this cell loses strength as the Richardson number increases. For another thermal conductivity ratio, the primary cell occupying the left chest is due to the movement of the lid in the anti-clockwise direction and the secondary cell is due to natural convection and this cell vanishes as the Richardson number increases. The primary cell becomes due to natural convection and the secondary cell becomes bigger owing to forced convection because the effect of forced convection becomes weaker when $\mathrm{Ri} = 10$. The isothermal lines distribution depends on the thermal conductivity ratio. By increasing this ratio, the temperature distribution becomes more uniform in the two chests because the partition becomes a highly conducive partition.

Figure 3 Comparison of the streamlines and temperature contours between the present work and that of Oztop et al. (2009b) for square cavity with downward moving lid of the left sidewall and different Richardson numbers: (a) Ri = 0.1; (b) Ri = 1 and (c) Ri = 10 at $K = 1$, $\mathrm{Gr} = 10^5$, $\mathrm{Pr} = 0.71$ and $Xp = 0.5$

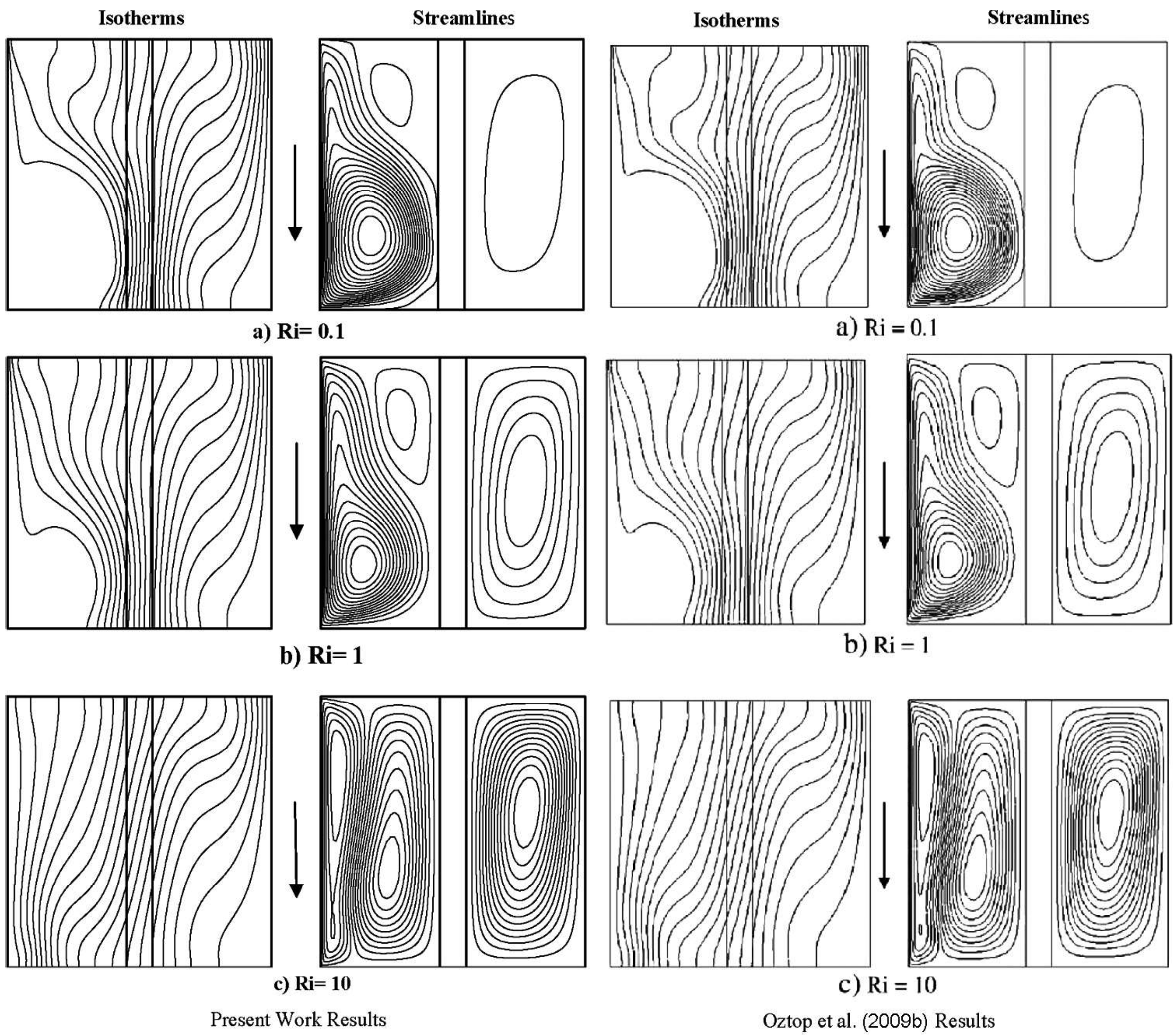

Figure 4 Isotherms (on the left) and streamlines (on the right) for the two cases of upward (on the upper) downward (on the lower) moving lid of the left sidewall at different Richardson numbers (Ri) and thermal conductivity ratios (K) with $\Phi = 0°$

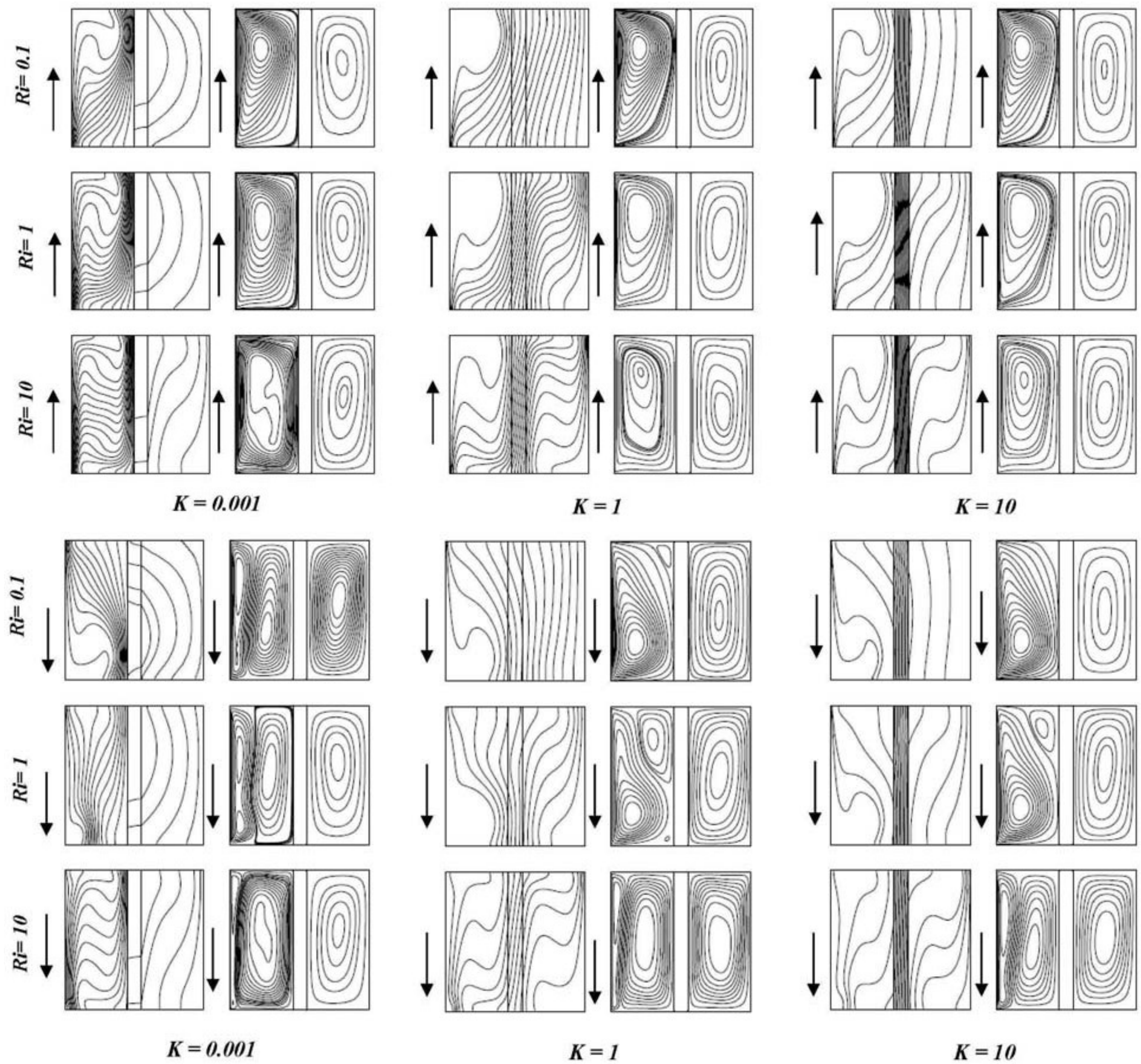

Figures 5 and 6 show the isotherms (on the left) and streamlines (on the right) for the two cases of upward and downward lid movement of the left side wall for different Richardson numbers (Ri), thermal conductivity ratios (K) and wall inclination angles from vertical direction (Φ). As mentioned previously, it can be seen from the streamline contours that positive values of (Φ) reduce the strength of the convective motion much more than negative values of (Φ). One can see in these figures that the flow structure spreads along the inclined chests and the combined convection appears clear when $\mathrm{Ri} = 1$ and the lid moves downward because of the opposite direction of flow between forced and natural convection. It is also evident that for ($\Phi = -60°$) that the convective cell is more elongated and penetrates deeper into the acute corners of the enclosure than for ($\Phi = 60°$). As a result, the temperature contours for ($\Phi = \pm 60°$) can be seen to be strikingly different. The buoyancy force is dominant when $\mathrm{Ri} >> 1$ and when heat transfer is primarily by free convection. The forced convection heat transfer becomes effective when $\mathrm{Ri} << 1$. For the low thermal conductivity ratio $K = 0.001$, the solid partition acts as an insulator between the hot and cold fluid streams. Little isotherms crossing the solid partition of lower K can be seen. Figure 7 displays the local Nusselt numbers for the case of upward lid-driven flow at different Richardson numbers, thermal conductivity ratios and wall inclination angles from the vertical direction (Φ). There are big differences between the cases for the trend of the local Nusselt numbers. These differences can be seen from the local Nusselt numbers along the moving wall. It is observed that the local Nusselt number decreases with increasing values of the thermal conductivity ratio for all values of the Richardson numbers. Figure 8 displays the local Nusselt number for the case of downward lid-driven flow at different Richardson numbers, thermal conductivity ratios and wall inclination angles from the vertical direction (Φ).

Figure 5 Isotherms (on the left) and streamlines (on the right) for the two cases of upward and downward moving lid of the left sidewall at different Richardson numbers (Ri), thermal conductivity ratios (K) and wall inclination angles from vertical ($\Phi = 30°$ and $\Phi = -30°$): (a) Case I, $\Phi = 30°$ and (b) Case II, $\Phi = -30°$

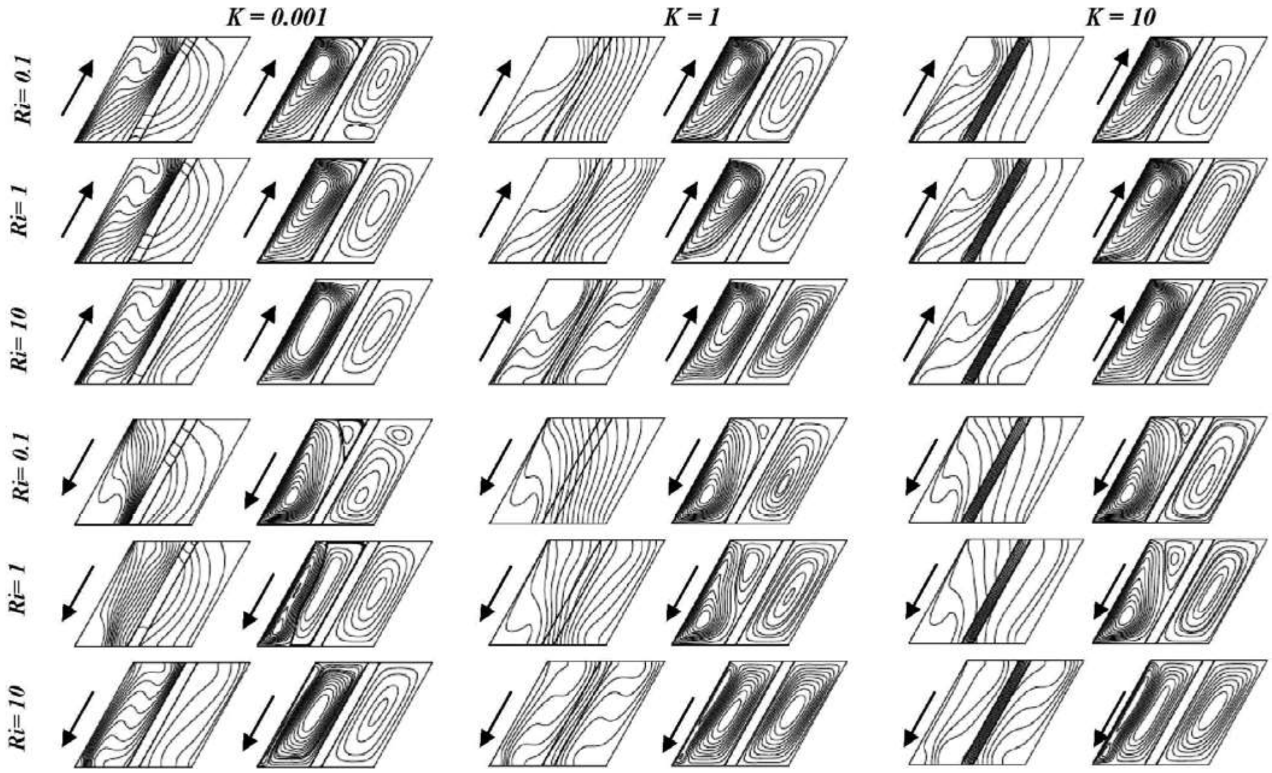

(a)

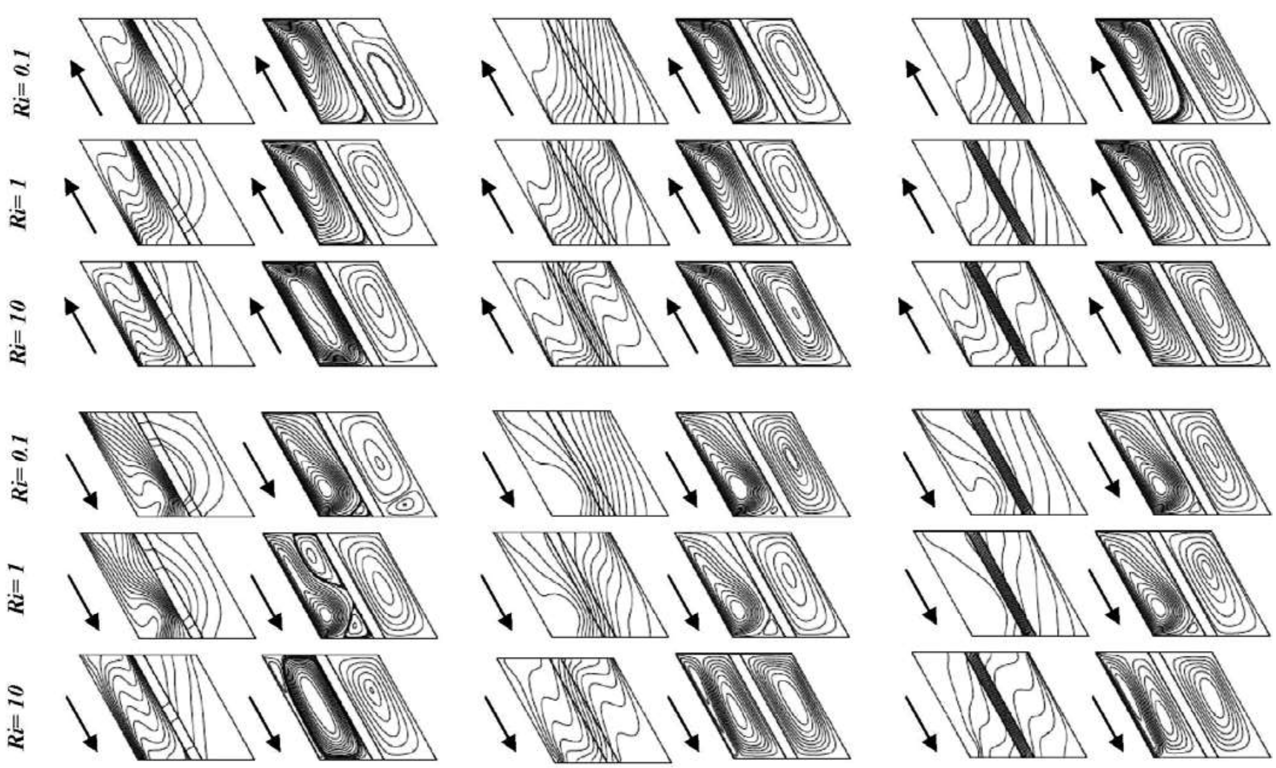

(b)

Figure 6 Isotherms (on the left) and streamlines (on the right) for the two cases of upward and downward moving lid of the left sidewall at different Richardson numbers (Ri), thermal conductivity ratios (*K*) and wall inclination angles from vertical ($\Phi = 60°$ and $\Phi = -60°$): (a) Case III, $\Phi = 60°$ and (b) Case IV, $\Phi = -60$

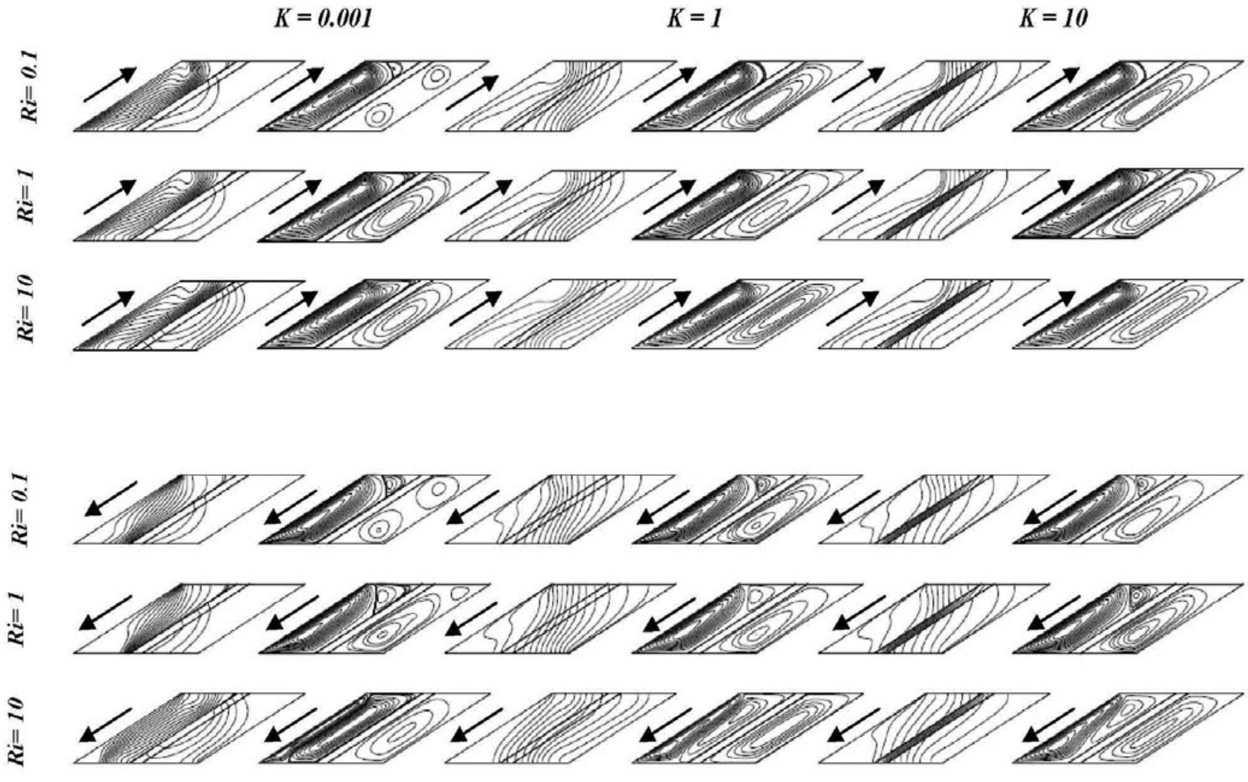

(a)

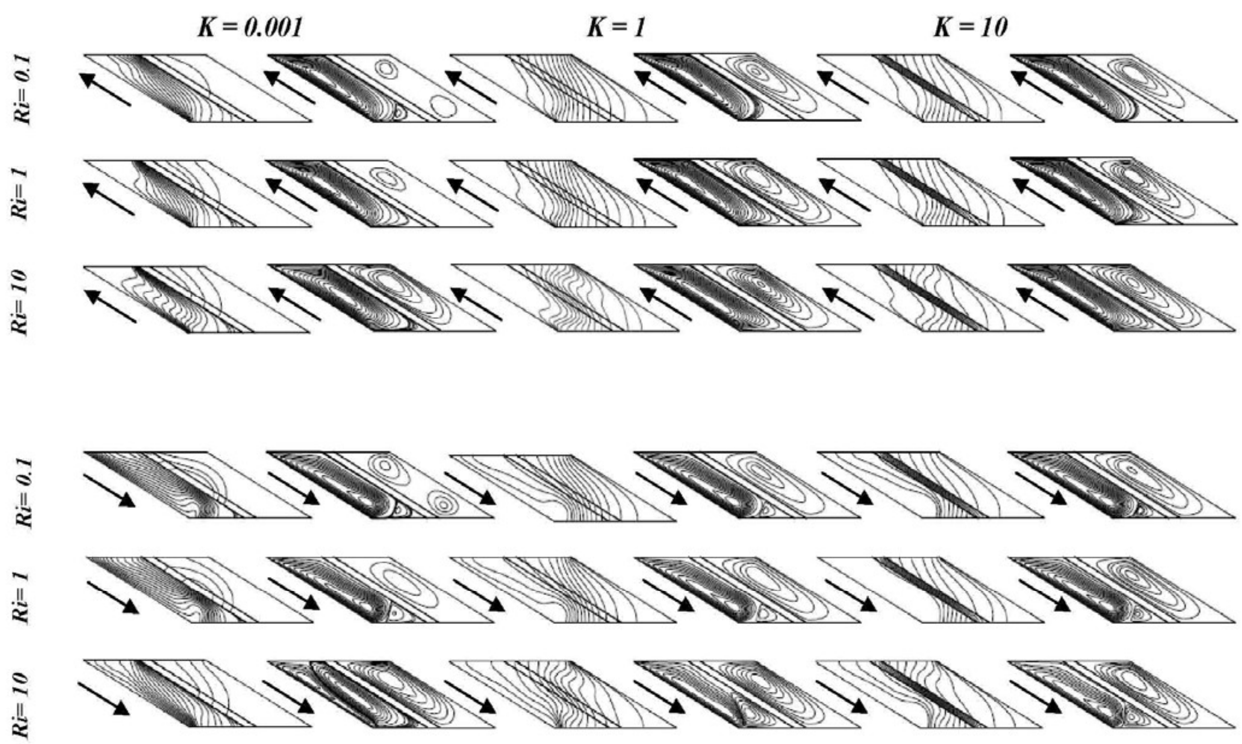

(b)

Figure 7 Local Nusselt number, Nu of moving left wall along *y*-axis for the case of upward lid driven with different thermal conductivity ratios (*K*) and wall inclination angles from vertical (Φ)

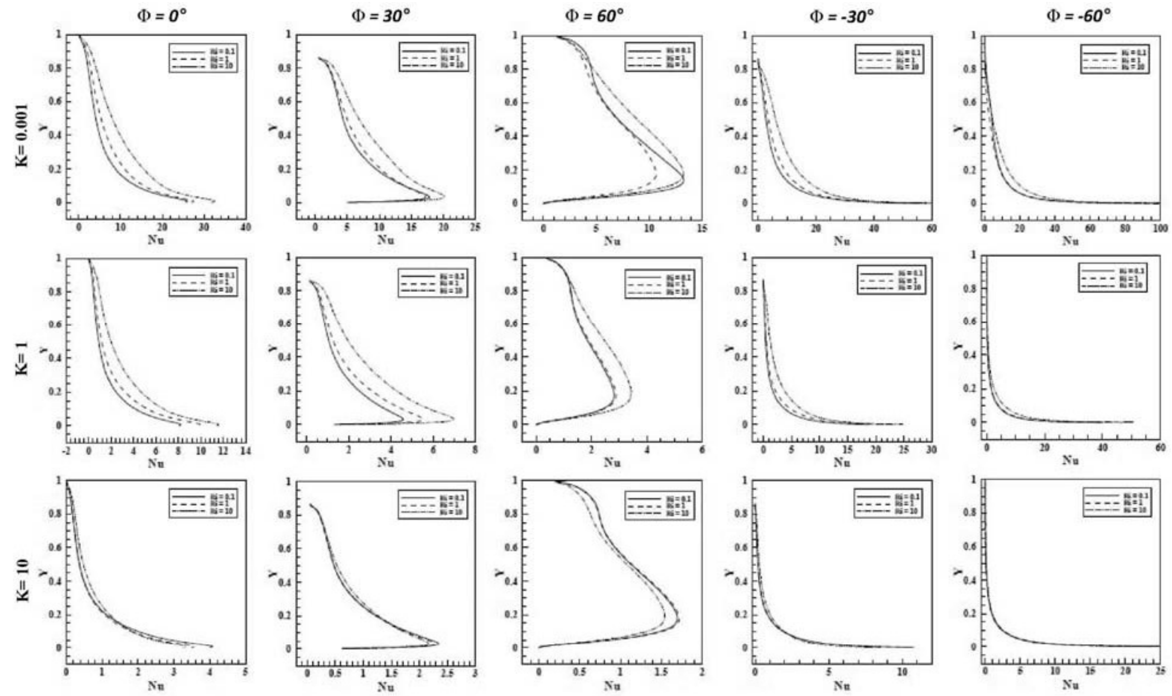

Figure 8 Local Nusselt number, Nu of moving left wall along *y*-axis for the case of downward lid driven with different thermal conductivity ratios (*K*) and wall inclination angles from vertical (Φ)

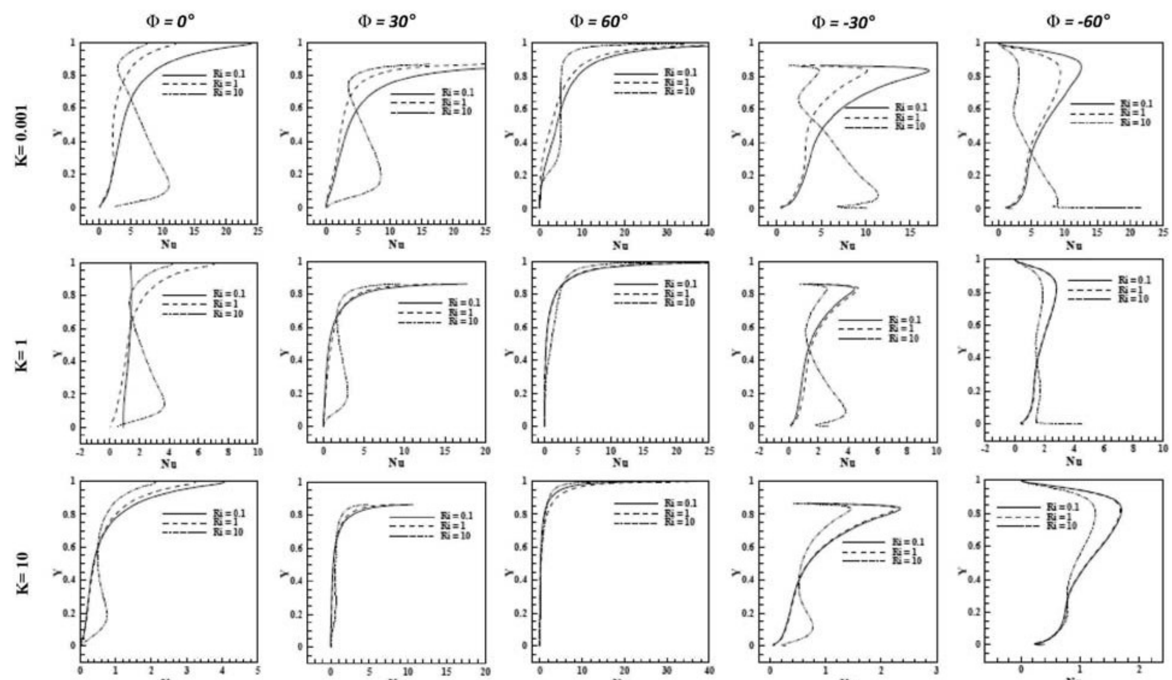

Figure 8 displays the local Nusselt number for the case of downward lid-driven flow at different Richardson numbers, thermal conductivity ratios and wall inclination angles from the vertical direction (Φ). The highest average Nusselt number is predicted at the highest Richardson number. Sinusoidal-shaped variation occurs at the highest Richardson number owing to the domination of natural convection heat transfer. In this case, the flow motion mostly occurs owing to buoyancy forces since the velocity of the moving lid is low. The heat transfer decreases with increasing values of the thermal conductivity ratio for all Richardson numbers.

Finally, Table 2 presents the mean Nusselt number along the moving wall for the two different lid movement cases. It is clearly seen that the maximum mean Nusselt number for the case of upward lid movement is predicted to be at $\Phi = -60°$ (Ri = 10, $K = 0.001$) while the maximum mean Nusselt number for the case of downward lid movement is obtained at $\Phi = -30°$ (Ri = 0.1, $K = 0.001$). On the other hand, the minimum mean Nusselt numbers for the two different cases (upward and downward lid movements) are predicted at $\Phi = 0°$. The variation of the average skin friction coefficient (C_f) with different angles of inclination, Richardson numbers and thermal conductivity ratios is plotted in Figure 9 for both downward and upward lid-driven cavities. In general, the average skin friction coefficient decreases with increasing the angle of inclination up to $\Phi = 0°$ and then increases with increasing the inclination angle. This fact can be noticed for all values of the Richardson number and thermal conductivity ratio considered except when the Richardson number is equal to 10 because of the increase in the moving wall velocity.

Table 2 Mean Nusselt number along moving wall for two different cases

Case	*Left wall Inclination angle from vertical* (Φ)	*Ri*	*Mean Nusselt number along moving wall*		
			K = 0.001	*K = 1*	*K = 10*
Upward moving lid	0°	0.1	2.8847800	2.0532500	0.6652500
		1	2.5724100	2.04102500	0.6558900
		10	2.2708500	1.8665800	0.6278400
	30°	0.1	6.5486960	1.6683315	0.8110626
		1	6.9601380	2.0198620	0.7984151
		10	8.9478650	2.8309550	0.8240597
	60°	0.1	7.3120580	1.7606860	1.0641250
		1	6.4677640	1.7954820	1.0720000
		10	7.9692650	2.1686550	0.9706705
	–60°	0.1	5.806804	1.487568	0.7899672
		1	6.9297490	1.8669950	0.7917060
		10	9.7859360	2.8165590	0.8211336
	–30°	0.1	6.7358612	1.4964390	0.9802706
		1	6.0313760	1.5791770	0.9965230
		10	8.6014620	2.1755920	0.9696504
Downward moving lid	0°	0.1	2.8453300	2.0443000	0.6778100
		1	2.0314200	1.7258400	0.6590500
		10	1.6421000	1.4223100	0.5586300
	30°	0.1	5.2289220	1.4309950	0.7857457
		1	3.0264300	1.4449910	0.6925970
		10	5.8702960	2.2370350	0.7425945
	60°	0.1	6.4027810	1.4831800	0.9764392
		1	4.9649600	1.4398700	0.9640152
		10	4.2778600	1.4731230	0.7971712
	60°	0.1	6.2459170	1.6481240	0.8129842
		1	4.2525280	1.8330950	0.8004820
		10	6.2778170	2.1693410	0.7298536
	30°	0.1	7.0215500	1.7583170	1.0656470
		1	5.8814610	1.7656540	1.0600690
		10	4.4145570	1.5440440	0.8825246

Figure 9 Variation of the average skin friction coefficient (C_f) of moving left wall along y-axis with wall inclination angles from vertical (Φ) for both cases of downward (dashed line) and upward (solid line) lid-driven cavities with different thermal conductivity ratios (K)

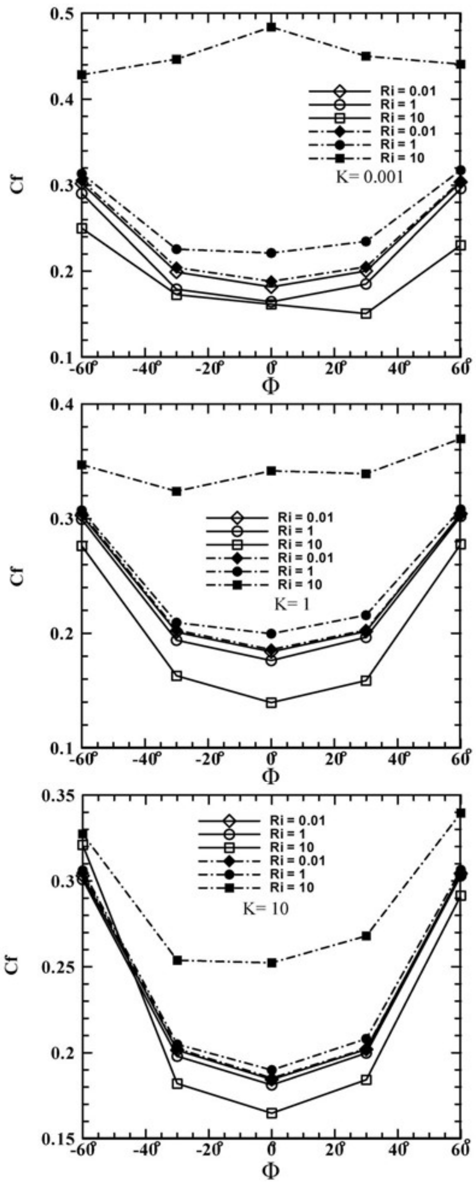

7 Conclusions

Laminar steady mixed convection and conduction in a differentially heated lid-driven parallelogram-shaped enclosure divided by a solid conductive partition with a finite length and thermal conductivity into two equal chests was simulated numerically using the finite-volume method. The inclined side walls of the parallelogram cavity were maintained at constant temperatures while its horizontal walls were thermally insulated. Two different cases were considered based on the direction of the lid movement of the left inclined side wall as downward or upward. The numerical procedure adopted in this study produced a consistent performance over a wide range of parameters. These were $0.1 \leq \text{Ri} \leq 10$, $-60° \leq \Phi \leq 60°$ and $0.001 \leq K \leq 10$. The results obtained in this study showed how the mean Nusselt number for a parallelogram-shaped enclosure varied with the wall angle Φ. For the upward lid movement case, positive values of Φ caused a greater reduction in the overall Nusselt number than the same negative value of Φ. Also, negative values of Φ produced a more uniform distribution of the local Nusselt number than positive Φ values. For the downward lid movement case, positive values of Φ produced a more uniform distribution of the local Nusselt number than negative Φ values. It was also predicted that the minimum mean Nusselt number for the two cases (upward and downward lid movement) occurred for $\Phi = 0°$. The mean Nusselt number decreased with increasing values of the Richardson number for all values of the thermal conductivity ratio. The heat transfer decreased with increasing values of the thermal conductivity ratio for all Richardson numbers. The flow characteristics and convection heat transfer inside the parallelogram-shaped enclosure depended strongly on the mixed convection parameter Ri, temperature gradient, movement of heat through the wall, and the wall inclination angle. Little isotherms crossing the solid partition were predicted for lower thermal conductivity ratios. The average friction coefficient (C_f) had minimum values at $\Phi = 0°$ for all values of the Richardson number considered except when Ri = 10. Also, the values of the average skin friction coefficient for an upward moving lid were predicted to be lower than those for a downward moving lid at all conditions.

References

Bairi, A., Garcia, J.M., Maria, D. and Laraqi, N. (2010) 'Transient natural convection in parallelogramic enclosure with isothermal hot wall, experimental and numerical study applied to on-board electronics', *Applied Thermal Energy*, Vol. 30, pp.1115–1125.

Ben Nakhi, A. and Chamkha, A. (2006) 'Natural convection in inclined partition enclosures', *J. Heat Mass Transfer*, Vol. 42, pp.311–321.

Costa, V.A.F. (2004a) 'Double-diffusive natural convection in parallelogramic enclosure filled with fluid saturated porous media', *Int. J. Heat and Mass Transfer*, Vol. 47, pp.2699–2714.

Costa, V.A.F. (2004b) 'Double-diffusive natural convection in parallelogramic enclosure', *Int. J. Heat and Mass Transfer*, Vol. 47, pp.2919–2926.

Costa, V.A.F., Oliveira, M.S.A. and Sousa, A.C.M. (2005) 'Laminar natural convection in a vertical stack of parallelogramic partial enclosures with variable geometry', *Int. J. Heat and Mass Transfer*, Vol. 48, pp.779–792.

Ferzinger, J. and Peric, M. (1999) *Computational Methods for Fluid Dynamics*, 2nd ed., Springer Verlag, Berlin.

Garcia, J.M., Maria, D., Bairi, A. and Costa, V.A.F. (2010) 'Empirical correlations at high Ra for steady-state convection in 2D air filled parallelogramic enclosure with isothermal discrete heat source', *Int. J. Heat and Mass Transfer*, Vol. 53, pp.3831–3838.

Jae, R.L. and Man, Y.H. (2006) 'Numerical simulation of natural convection in a horizontal enclosure with a heat-generating conducting body', *Int. J. Heat and Mass Transfer*, Vol. 49, pp.2684–2702.

Liaqat, A. and Baytas, A.C. (2001) 'Conjugate natural convection in a square enclosure containing volumetric sources', *Int. J. Heat and Mass Transfer*, Vol. 44, pp.3273–3280.

Mahapatra, S.K., Sarkar, A. and Sarkar, A. (2007) 'Numerical simulation of opposing mixed convection in differentially heated square enclosure with partition', *Int. J. Thermal Science*, Vol. 46, pp.970–979.

Nakumura, H. and Asako, Y. (1980) 'Heat transfer in parallelogram shaped enclosure', 1st Report, *Bulletin of the JSME*, Vol. 23, pp.1827–1834.

Nakumura, H. and Asako, Y. (1982) 'Heat transfer in parallelogram shaped enclosure', 2nd Report, *Bulletin of the JSME*, Vol. 25, pp.1412–1418.

Nakumura, H. and Asako, Y. (1984) 'Heat transfer in parallelogram shaped enclosure', 4th Report, *Bulletin of the JSME*, Vol. 27, pp.1144–1151.

Naylor, D. and Oosthuizen, P.H. (1994) 'A numerical study of free convective heat transfer in a parallelogram-shaped enclosure', *Int. J. Num. Heat Fluid Flow*, Vol. 4, pp.553–559.

Oztop, H.F. and Varol, A. (2009) 'Combined convection in inclined porous lid-driven enclosure with sinusoidal thermal boundary condition on one wall', *Progress in Computational Fluid Dynamic*, Vol. 9, pp.127–131.

Oztop, H.F., Varol, Y. and Koca, A. (2009c) 'Natural convection in a vertically divided square enclosure by a solid partition into air and water regions', *Int. J. Heat and Mass Transfer*, Vol. 52, pp.5909–5921.

Oztop, H.F., Zhao, Z. and Yu, B. (2009a) 'Fluid flow due to combined convection in lid-driven enclosure having circular body', *Int. J. Heat and Fluid Flow*, Vol. 30, pp.886–901.

Oztop, H.F., Zhao, Z. and Yu, B. (2009b) 'Conductive-combined forced and natural convection in lid-driven enclosures divided by a vertical solid partition', *Int. Comm. Heat and Mass Transfer*, Vol. 36, pp.661–668.

Patankar, S.V. (1980) *Numerical Heat Transfer and Fluid Flow*, McGraw-Hill, New York.

Rahman, M.M., Alim, M.A., Saha, S. and Chowdhury, M.K. (2008) 'A numerical study of mixed convection in a square cavity with a heat conducting square cylinder at different locations', *Journal of Mechanical Engineering ME39, Transaction of the Mech. Eng. Div.*, The Institution of Engineers, Bangladesh, pp.78–85.

Stone, H.L. (1968) 'Iterative solution of implicit approximations of multidimensional partial differential equations', *SIAM J. Num. Analysis*, Vol. 5, pp.530–558.

Varol, Y., Oztop, H.F. and Koca, A. (2010) 'Effects of inclination angle on conduction-natural convection in divided enclosures filled with different fluids', *Int. Comm. Heat and Mass Transfer*, Vol. 37, pp.182–191.

WanLai, L., Carlson, K.D. and Cing-Jen, C. (1997) 'Pressure boundary conditions of incompressible flows with conjugate heat transfer on non-staggered grids', *Numerical Heat Transfer*, Vol. A32, pp.459–479.

Zhao, F.Y., Liu, D. and Tang, G. F. (2010) 'Determining boundary heat flux profiles in an enclosure containing solid conducting block', *Int. J. Heat and Mass Transfer*, Vol. 53, pp.1269–1282.

Nomenclature

Symbol	*Description*
C_f	Average skin friction coefficient
g	Gravitational acceleration (m/s^2)
Gr	Grashof number
H	Height of the enclosure (m)
K	Fluid-solid thermal conductivity ratio
k	Thermal conductivity of fluid (W/m °C)
k_S	Thermal conductivity of solid wall (W/m °C)
L	Width or height of the enclosure (m)
$\overline{\mathrm{Nu}}$	Average Nusselt number
P	Dimensionless pressure
p	Pressure (N/m^2)
Pr	Prandtl number
Ri	Richardson number
Re	Reynolds number
S	Thickness of partition (m)
T	Temperature (°C)
T_c	Temperature of the cold surface (°C)
T_h	Temperature of the hot surface (°C)
T_s	Temperature of solid partition surface (°C)
U	Dimensionless velocity component in x-direction
u	Velocity component in x-direction (m/s)
V	Dimensionless velocity component in y-direction
V_P	Lid-driven left wall velocity
V	Velocity component in y-direction (m/s)
W	Width of the enclosure (m)
X	Dimensionless coordinate in horizontal direction
X	Cartesian coordinate in horizontal direction (m)
Y	Dimensionless coordinate in vertical direction
Y	Cartesian coordinate in vertical direction (m)
Greek symbols	
α	Thermal diffusivity (m^2/s)
β	Volumetric coefficient of thermal expansion (1/°C)
θ	Dimensionless temperature
θ_s	Dimensionless temperature of the solid partition
Φ	Sidewall inclination angle from vertical (degree)
ϑ	Kinematic viscosity of the fluid (m^2/s)
ρ	Density of the fluid (kg/m^3)